British Journal of Medicine & Medical Research
3(4): 1659-1670, 2013

SCIENCEDOMAIN *international*
www.sciencedomain.org

Cerebral FDG Metabolic Pattern in Pediatric Patients with Neurofibromatosis Type 1: A Retrospective Study

Nghi C. Nguyen[1*], Kaveh Vejdani[1] and Thomas J. Geller[2]

[1]Department of Radiology, Saint Louis University, Missouri, USA.
[2]Department of Neurology, Saint Louis University, Missouri, USA.

Authors' contributions

This work was carried out in collaboration between all authors. Author NCN designed the study, performed the data analysis and wrote the first draft of the manuscript. Author KV performed the data analysis and helped with manuscript preparation. Author TJG provided clinical information on the NF1 subjects, contributed to the study design and final version of the manuscript. All authors read and approved the final manuscript.

Research Article

Received 25th March 2013
Accepted 14th May 2013
Published 18th May 2013

ABSTRACT

Aims: Learning disabilities represent the most significant cause of lifetime morbidity in neurofibromatosis type 1 (NF1) patients. The cognitive phenotype of NF1 pediatric patients is not well understood. The purpose of this study was to examine the cerebral glucose metabolic pattern in NF1 pediatric patients.
Study Design: Retrospective.
Place and Duration of Study: Saint Louis University Hospital, Saint Louis, Missouri, United States, between May 2011 and May 2012.
Methodology: Six NF1 pediatric patients underwent FDG PET/CT including the brain, for evaluation of extracranial neoplasm. Their brain PET images were compared with a pediatric comparison set (21 subjects) using Statistical Parametric Mapping. Significant differences between groups were examined at $p<0.001$, uncorrected for voxel height and $p<0.05$, corrected for cluster extent.
Results: Compared with the comparison set, the 6 NF1 patients showed the largest cluster of reduced FDG uptake (3966 voxels) in the medial dorsal nucleus of bilateral thalami. Additional clusters of metabolism in the range from 415 to 926 voxels were

**Corresponding author: Email: nguyenn@slu.edu;*

noticed in the right cingulate gyrus (Brodmann area (BA) 8 and 24), left occipital lobe (BA 17 and 18) and right fronto-parietal lobe (BA 43).
Conclusion: The FDG reduction of the bilateral thalami is compelling and may be most pathognomonic for NF1. This and other areas of FDG reduction found within the brain may contribute to a better understanding of the NF1 cognitive phenotype.

Keywords: Neurofibtomatosis type 1; learning disabilities; pediatric patients; cerebral FDG PET; statistical parametric mapping.

1. INTRODUCTION

Neurofibromatosis type 1 (NF1) is a neurocutaneous disorder with a prevalence of approximately 1 in 3000 [1]. Patients with NF1 usually show intelligence quotient (IQ) levels in the low-average range (mean full-scale IQ of 90.6), with a shift to the left of the normal distribution [2]. Mental retardation in NF1 children (4-8%) is about twice as high as the general population [2]. Despite the low frequency of global mental retardation in patients with NF1, learning disabilities represent the most significant cause of lifetime morbidity in NF1 patients. Learning disabilities and school failure are the most common complications of NF1 in childhood, comprising 35-65% of the cases [3]. North et al. [3] found that 65% of NF1 children performed below chronologic age and 45% of them required special education assistance between the ages of 8 and 16 years. Hyperintense lesions on T2 weighted MR images (so called unidentified bright objects, UBOs) are pathognomonic of NF1 and may correlate with the risk of learning disabilities [4]. Increasing evidence suggests a correlation between dysregulation of Ras activity and learning deficits in NF1 [5-6].

Two cerebral FDG PET studies in NF1 pediatric patients have been published. Kaplan et al. [7] performed FDG PET in 10 NF1 children, aged 4–15 years. Thalamic uptake was found to be reduced by about 35% in the NF1 children compared to controls. In addition, the FDG uptake was decreased in areas with large UBOs, and there were varying degrees of FDG reductions in the cortex in all NF1 children. Balestri et al. [8] performed FDG PET in four NF1 subjects, aged between 10 and 20 years, who had UBOs and neurological symptoms, including seizures, as well as language disabilities and mental retardation. There was widespread hypometabolism not related to the localization of MRI abnormalities in three of the four subjects.

The cognitive FDG phenotype of NF1 pediatric patients is complex and poorly understood because of the paucity of reports and the limitations related to study design and image analyses. In the current study, voxel-based statistical parametric mapping (SPM) is being applied for the first time to examine the cognitive phenotype in NF1 pediatric patients.

2. MATERIALS AND METHODS

2.1 Patients

A review of FDG PET/CT reports between June 2004 and December 2009 identified 6 pediatric patients (5 male, 1 female, median age 14 years, range 6-18) with history of NF1 who underwent PET/CT scanning for characterization, staging and restaging of extracranial neoplasm. Their medical records including treatment modalities and neurological symptoms as well as cognitive function were reviewed. Only two of six NF1 patients had recent MRI of

the brain. We therefore decided not to evaluate the MRI scans to correlate with the PET findings. The institutional review board approved this retrospective study.

2.2 FDG PET/CT Scanning

All patients fasted at least 4 hours before the PET/CT examination and received an IV injection of approximately 5.18 MBq/kg of body weight of FDG, with a maximum dose of 444 MBq (12 mCi). The median blood glucose concentration immediately before tracer injection was 97 mg/dL (range 83-108) in the 6 NF1 patients and 92 md/dL (range 76-119) in the 21 subjects that served as comparison set. Study subjects sat in a quiet room where the injection took place and were instructed not to talk during the subsequent FDG uptake phase with a median of 62.5 minutes (range 50-70) in the NF1 subjects and 64 minutes (range 49-83) in the comparison set. The whole-body scans from top of the head to the feet, which is the standard PET/CT acquisition protocol at our institution for oncological indications, were acquired on a PET/CT scanner (Gemini TF, Philips Healthcare). PET scans were acquired at 1.5 or 2.0 minutes per bed position depending on the patient's weight with a 50% overlap. Dedicated PET of the brain was not performed. The study subjects were not given any specific instructions about whether to open or close their eyes during PET/CT scanning. The CT data were used for image fusion and the generation of the CT transmission map. This retrospective study was approved by the Institutional Review Board and patients' informed consent was waived.

2.3 Image Analysis

The brain PET images of the NF1 subjects were extracted from the whole-body scan using the MIMneuro 4.1 software (MIMvista Corp., Cleveland, OH). The PET images were transferred to the Statistical Parametric Mapping (SPM) software (SPM8, Wellcome Department of Cognitive Neurology, University College London, UK) for statistical analyses, implemented via Matlab 7.12.0 (Mathworks, Natick, MA, USA).

A comparison set consisting of 21 pediatric patients (10 male, 11 female, median age 16, range 3-18) were randomly selected out of a collection of 33 pediatric patients undergoing PET/CT (Gemini TF, Philips Healthcare) at our institution for extracranial neoplasm not related to NF1 (17 lymphomas and 1 neuroblastoma, malignant melanoma, rhabdomyosarcoma as well as Ewing's sarcoma each). Their brain PET images were loaded into SPM8 the same way as for the NF1 subjects. Their PET/CT imaging protocol was identical with that of the NF1 subjects in the current study. They did not have a history of brain tumor, neuropsychological disease, or chemotherapy prior to PET/CT.

The PET images were spatially normalized to match the standard stereoanatomic space using a 12-parameter affine (linear) transformation, followed by a nonlinear transformation with a basis function of 4 x 5 x 4. Global counts were normalized by proportional scaling to remove confounding effects due to global changes, and smoothed with a fullwidth half maximum (FWHM) Gaussian kernel of 6 mm. The voxel size was 2 x 2 x 2 mm and the FWHM was 17.0 x 16.6 x 16.4 mm. A two-sample t test was performed for the hypothesis that the NF1 subjects show reduced uptake compared with the comparison set (NF1 < comparison set). The significant differences between the two groups were examined at $p<0.001$, uncorrected for voxel height, and $p<0.05$, corrected for cluster extent using family-wise-error correction for multiple comparisons [9]. We used the software GingerALE 2.1.1 to convert the MNI coordinates derived from SPM8 into Talairach space [10]. Subsequently, the software Talairach Client 2.4.2 was used to assign brain regions (Talairach atlas) for a

given x,y,z Talairach coordinate [11]. The assigned label is hierarchical, and is composed of five levels: hemisphere, lobe, gyrus, tissue type, and cell type. The Talairach atlas for the nearest gray matter within 11 mm of the local maxima was searched.

3. RESULTS

3.1 Case Presentation

3.1.1 Case #1

This 15-year old boy was diagnosed with NF1 as an infant and had a pelvic rhabdomyosarcoma as a toddler. His PET/CT study was performed at the age of 13 years and 11 months and showed local tumor recurrence. Developmental and cognitive findings as well as academic achievements remained entirely normal. A MRI of the brain was performed at the age of 13 because of migraine headaches and showed normal brain findings.

3.1.2 Case #2

The 18-year old boy was diagnosed with NF1 at the age of 9. He had some speech and language problems at the time of initial diagnosis but demonstrated normal academic achievements and cognitive function since the age of 13. This was based on school reports of testing and he received no additional assistance academically in middle school and high school. The PET/CT study was performed at age 17 years and 6 months for further evaluation of bone lesions in the lower extremities.

3.1.3 Case #3

The 15-year-old girl with history of NF1 represented with a left shoulder mass associated with subacute pain. MRI showed a 3-cm contrast enhancing mass in the area of the left brachial plexus. In addition, there were multiple non-enhancing soft tissue lesions along the C-spine suggestive of plexiform neurofibromas. The subsequent FDG PET/CT exam showed moderate uptake within the left shoulder mass which was thought to be low to intermediate grade tumor. The paracervical soft tissue lesions were not FDG avid and thus most likely benign. Developmental and cognitive findings as well as academic achievements appeared normal.

3.1.4 Case #4

This 6-year old boy with NF1 developed significant thoracic scoliosis with a plexiform appearing tumor of his right paraspinal cervical region. The progressive back pain was unresponsive to simple analgesics, gaba-pentin and nortryptaline. PET/CT was performed at the age of 5 years and 9 months for further characterization and pre-operative staging of the paraspinal tumor. Cognitive function was age-appropriate but he had a learning disability seen as delays in expressive and written language that have improved in kindergarten. Formal neurocognitive testing has been requested but not completed.

3.1.5 Case #5

This 18-year old patient was diagnosed with NF1 as an infant. He developed a malignant peripheral nerve sheath tumor of the thigh at the age of 15. He had normal cognitive function

until school age. He then developed specific learning disabilities that required reading and mathematics assistance since his third grade. His intelligence was reported to be normal. The PET/CT study was performed at the age of 18 years and 0 months for restaging of malignant peripheral nerve sheath tumor 2 months after chemotherapy.

3.1.6 Case #6

This 13-year old NF1 patient demonstrated progressive optic pathway tumor that required stereotactic radiosurgery of the chiasm at age of 7. He had 20/250 and 20/400 corrected vision. Two Gadolinium-enhancing lesions of 1 cm right thalamus and right cerebellum at MRI remained stable in size for at least 2 years. The PET/CT study at the age of 12 and 4 months was performed for further evaluation of a soft tissue lesion in the left hand. The lesions in the right thalamus and right cerebellum did not demonstrate increased FDG uptake. Also, they did not affect the brain metabolism because the metabolism was symmetric in both brain hemispheres on visual evaluation and by using L/R% indices. Cognitive function remained in the low normal range but he was found to have learning disabilities requiring occupational, physical, and speech therapy.

3.2 Image Analysis

Compared with the comparison set, the 6 NF1 pediatric patients showed 4 clusters of hypometabolism in the range from 415 to 3966 voxels. A total of 12 voxel peaks > 8 mm apart were found within these 4 clusters (Table 1). Six of 12 voxel peaks matched exactly (range 0 mm) to the corresponding Brodmann areas (BA). The remaining 6 voxel peaks were located within 1-5 mm from the nearest BA. The BA was available for 11 of 12 voxel peaks. For only 1 voxel peak, localized left occipital lobe, the BA could not be specified by the software Talairach Client.

Table 1. SPM results of all 4 clusters. Peak locations within the clusters are > 8 mm apart; the T values, Talairach coordinates and Brodmann areas as well as distance (in mm) to the nearest gray matter are shown. * Brodman area not specified by Talairach Client

Cluster Level		Voxel Level	Talairach Coordinates (mm)			Brain Region	Brodmann Area (BA)	Distance (mm)
Cluster Size	P_{cor}	T value	X	Y	Z			
3966	<0.0001	5.8	5	-17	5	R thalamus, medial dorsal nucleus	Medial Dorsal Nucleus	0
		5.6	13	-20	13	R thalamus, medial dorsal nucleus	Medial Dorsal Nucleus	0
		5.4	-6	-21	11	L thalamus	Medial Dorsal Nucleus	0
926	0.001	5.1	11	6	36	R cingulate gyrus	BA 24	0
		4.8	12	0	42	R cingulate gyrus	BA 24	1
		4.6	12	26	45	R frontal lobe, medial frontal gyrus	BA 8	2
627	0.009	5.1	-13	-93	-1	L occipital lobe, lingual gyrus	BA 17	0
		4.9	-15	-85	-8	L occipital lobe, lingual gyrus	BA 18	2
		4.4	-19	-81	-15	L occipital lobe, lingual gyrus	*	1
415	0.043	5.2	-47	-11	22	L parietal lobe, postcentral gyrus	BA 43	5
		4.9	-58	-9	20	L parietal lobe, postcentral gyrus	BA 43	0
		4.2	-61	-4	14	L frontal lobe, precentral gyrus	BA 43	1

The largest cluster of 3966 voxels was confined to the medial dorsal nucleus of the bilateral thalamus (Fig. 1). In addition to the SPM results, Fig. 2 represents actual PET images, showing the marked FDG reduction within the bilateral thalami of a NF1 patient (Case #5) compared to a subject from the comparison set.

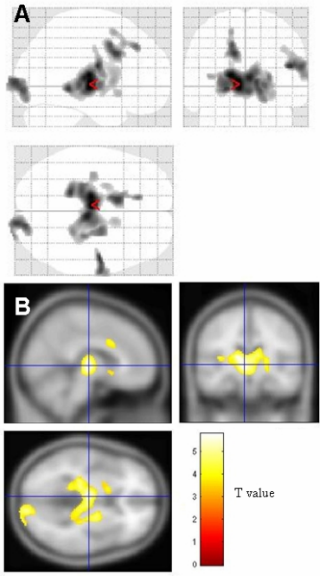

Fig. 1. A, SPM superimposes a maximum intensity projection (MIP) image on a glass brain in three orthogonal planes (height threshold for T = 3.45, p < 0.05). The pointing angle shows the cluster within the medial dorsal nucleus of the right thalamus. B, MIP is superimposed onto a T1-weighted template in three orthogonal planes within the standardized space. Crosshair shows a cluster within the right thalamus

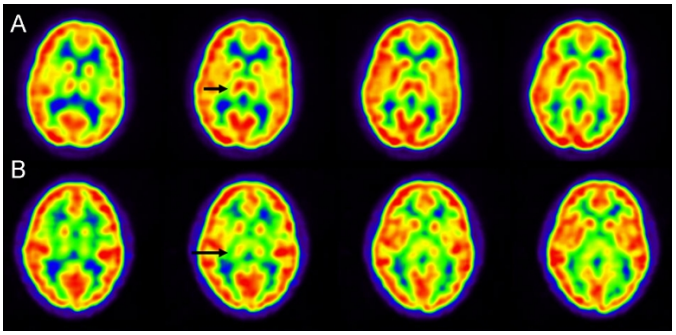

Fig. 2. Consecutive axial slices through the basal ganglia of a comparison set subject and a NF1 patient. A, 17-year-old male patient with a history of Hodgkin's lymphoma of the mediastinum and right supraclavicular region. The thalamic uptake is normal and symmetric (short arrow), showing comparable uptake intensity to the striatum. B, 18-year-old male patient with NF1 (Case #5) who was diagnosed with NF1 as an infant. He developed specific learning disabilities since his third grade and required reading and mathematics assistance. The bilateral thalamic uptake (long arrow) is markedly reduced compared to that of the striatum

The 3 remaining clusters were distinctively smaller, containing 926 voxels in the right cingulate gyrus (Fig. 3) and nearby medial frontal gyrus (BA 8 and 24), 627 voxels in the left occipital lobe (BA 17 and 18), as well as 415 voxels in the left fronto-pariatal lobe (BA 43). Eleven clusters within 124 to 317 voxels were excluded from further interpretation because they were not statistically significant (p>0.05, corrected).

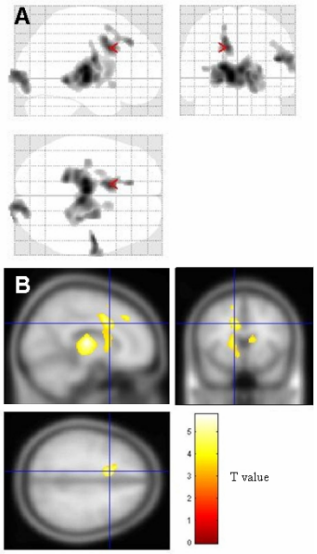

Fig. 3. A, SPM superimposes a maximum intensity projection (MIP) image on a glass brain in three orthogonal planes (height threshold for T = 3.45, p < 0.05). The pointing angle shows the cluster within the right cingulate gyrus (Brodman area 24). B, MIP is superimposed onto a T1-weighted template in three orthogonal planes within the standardized space. Crosshair shows a cluster within the right cingulate gyrus

4. DISCUSSION

4.1 Case Presentation

Three NF1 patients (Case #1-3) presented with normal academic achievements and intelligence. The other 3 NF1 patients (Case #4-6) were noted to have learning disabilities but their intelligence was either normal or low normal. These findings represent the well-documented cognitive features in NF1 pediatric patients [2,3].

4.2 Image Analysis and Interpretation

Our findings concur with previous PET studies performed in pediatric NF1 patients [7,8]. Kaplan et al. [7] performed FDG PET in 10 pediatric NF1 patients and found that their thalamic FDG uptake was reduced by about 35% compared with control subjects. Balestri et al. [8] also found bilateral thalamic hypometabolism in 3 of 4 NF1 pediatric patients. The current study of six NF1 pediatric patients reveals a very large cluster of FDG reduction (3966 voxels) within the bilateral thalami, which is consistent with a recent report by Burchert et al. for adult NF1 patients [12]. They found a large cluster of 1450 voxels within the bilateral thalami based on the same 2x2x2 mm voxel size as in the current study. The larger thalamic cluster found in the current study may fit with the previous hypothesis that the

thalamic FDG reduction may be more severe in pediatric than adult NF1 patients, approximately 35% vs. 8% [7,12]. This may reflect a functional recovery of the thalamus metabolism with age, which may be encountered not only in NF1 subjects but also in healthy subjects [13].

Our study represents the first SPM data on pediatric NF1 subjects and is able to pinpoint the area of hypometabolism within the thalamus – the medial dorsal nucleus. In a recent study using image fusion of ultrahigh-resolution PET and ultrahigh-field 7T MRI, the medial dorsal nucleus demonstrates the highest FDG uptake among various thalamic nuclei in all 5 healthy volunteers [14]. It is one of the largest thalamic nuclei and has been associated with working memory as it has reciprocal connections with the prefrontal association cortex [15]. It plays an important role in attention, decision-making, language comprehension, and active memory. Therefore, our findings further support and extend the hypothesis that thalamic hypometabolism, specifically within the medial dorsal nucleus, is pathognomonic for NF1 pediatric patients [7,12]. Potentially, the FDG hypometabolism may be more severe in subjects with cognitive impairment than those without, but a prospective study with neuropsychological assessment would be required to allow a correlation between the degree of FDG reduction and cognitive function.

In addition to the findings of the thalamus, we found large clusters within the right cingulate gyrus (BA 24) and nearby medial frontal gyrus (BA 8), the left occipital lobe (BA 17, 18) and left fronto-parietal lobe (BA 43). The left occipital lobe hypometabolism may coincide with the well documented deficits in visual-spacial processing in NF1 children [16]. Our findings also concur with the observed FDG reduction in the occipital and parietal lobe in 3 of 4 subjects and in the frontal cortex in 2 of 4 subjects by Balestri et al. [8].

In another neurocognitive context, Herholz et al. [17] found that the activation of the pre- and postcentral gyrus (BA 43) seemed to correspond with the task of naming the face in adult subjects undergoing cerebral O-15 water PET activation studies although this pattern of brain activation may not be related to memory functions [17]. Possibly, the increased prevalence of difficulty of face recognition in the NF1 population may have a metabolic correlate within the BA 43 as well [18].

Hazlett et al. [19] found hypometabolism within the cingulate gyrus (BA 24) in autistic adults undergoing verbal memory tests and FDG PET scanning. Indeed, autistic patients have a 100 to 190-fold increased risk of neurofibromatosis; it has been suggested that autism and neurofibromatosis may share a genetic etiological factor [20,21]. No NF1 subject was diagnosed with autism; nevertheless, the observed hypometabolism within BA 24 might be pathognomonic in NF1 patients.

Our results and those of previous PET studies are hampered by the small sample size and huge methodological differences. Balestri et al. (8) reported widespread hypometabolism in three of four adolescents with NF1. One limitation is that all 9 age-matched control subjects in that study presented with some form of neurological disturbance including seizure, developmental disability or headache. In contrast, none of the normal controls in our study has evidence of neurological symptoms or disorders. Kaplan et al. [7] found varying FDG hypometabolism in the cortex of NF1 children. The semi-quantitative PET evaluation based on region-of-interest placements however was confined to areas with UBOs and adjacent normal brain tissue, that is, the thalamus, striatum, brain stem and some white matter regions.

The potential relationship between the UBOs and cognitive impairments in NF1 remains controversial, as to what extent they are involved in cognitive impairments. Several studies have found a relationship between cognitive impairments and the presence of UBOs [22-24]. Other studies have found no association between UBOs and cognitive function [25,26]. It cannot be excluded that some areas of hypometabolism may be associated with UBOs in the current study.

Ideally, a pediatric SPM template should be used to assess pediatric functional data such as the current study. However, an adult normal template can be used as an alternative when obtaining normal pediatric PET data is not feasible due to ethical constraints [27]. Muzick et al. [27] has shown in a study of 13 children that the spatial normalization of pediatric brains to an adult normal template results in a higher level of artifacts than in adult subjects. These artifacts however don't seem to affect the SPM analyses for children ages 6 years and older compared to those younger than 6 years. In the current study, none of the 6 NF1 subjects were younger than 6 years old. It is therefore unlikely that our findings have been affected by significant artifacts.

We chose the small full-width half maximum (FWHM) with a Gaussian kernel of 6 mm considering that pediatric brain images were being evaluated in which the brain structures are relatively small when compared to those derived from adult subjects. While spatial smoothing may improve signal-to-noise ratio and compensate for functional anatomical variability, a large smoothing kernel (e.g., 10 mm or larger) may loose smaller clusters [28].

Theoretically, reduced cortical volume could cause an apparent decrease in FDG uptake because of recovery effects related to the limited spatial resolution of the PET scanning [29]. However, the cortical volume is often increased in NF1 subjects [30], indicating that the observed hypometabolism in the current NF1 patients likely represents decreased cellular activity and not a recovery effect.

Some variations in blood glucose concentrations remain although all NF1 subjects showed blood glucose concentration < 150 mg/dL before tracer injection. These blood glucose variations, however, might have little impact on the SPM analysis because the brain images of the NF1 subjects were first normalized to remove confounding effects. Nonetheless, intensity normalization may be adversely affected when large areas of FDG reduction are present, resulting in artefactual increases or decreases in normal tissue [27].

The comparison set consisting of 21 subjects in the current study appears appropriate for statistical FDG PET analysis [31]. Although one subject is only 3 years old, the remaining 20 subjects are 6 years and older, which is consistent with the age of NF1 subjects. In our study, the brain images were extracted from the whole-body PET scanning, acquired at 1.5 or 2.0 minutes per bed position. This acquisition protocol had been tested before and showed almost equivalent outcomes to an acquisition protocol dedicated to the brain [32].

4.3 Limitations

We acknowledge the limitations of the small sample size and the retrospective nature of the study. Statistical differences seen in the SPM analysis might be caused by large variations in the measurements. Nonetheless, the SPM findings are compelling and of clinical interest considering the limited reports of FDG PET on NF1 cognitive function. Selective neuropsychological testing is beyond the aim of this study; a causative relation between

location of the hypometabolism and the type of specific learning disabilities cannot be properly evaluated in the present series.

Medical treatment such as analgesics and antidepressants may affect the brain metabolism [33,34]. Treatment with these drugs however is less likely to cause the distinct clusters which are consistent with previous reports. The patient in Case #6 had an optic pathway tumor that required radiosurgery. However, the right thalamic and right cerebellar lesions have remained stable in size at MRI for at least 2 years. Also, these lesions did not show focally increased or decreased FDG uptake and did not affect the overall brain metabolism based on visual evaluation. Nevertheless, it cannot be excluded that the brain lesions may cause subtle metabolic cerebral changes which remain undetected with the methods being used.

5. CONCLUSION

The striking FDG reduction of the bilateral thalamus in the NF1 subjects is consistent with previous studies and may be most pathognomonic for the NF1 cognitive phenotype. This and other areas of FDG reduction within the occipital lobe and cingulate as well as premotor and postmotor gyrus may contribute to a better understanding of the complex cognitive phenotype in NF1 patients. The findings need to be further investigated in a large study and formal neuropsychological assessment as well as anatomical imaging should be included to allow a proper characterization of the various cognitive impairments.

CONSENT

This retrospective study was approved by the Institutional Review Board and patients' informed consent was waived.

ETHICAL APPROVAL

This retrospective study was approved by the Institutional Review Board, Saint Louis University, IRB #21622.

COMPETING INTERESTS

No research support was granted. The authors report no conflict of interest.

REFERENCES

1. Friedman JM. Epidemiology of neurofibromatosis type 1. Am J Med Genet. 1999;89:1–6.
2. North KN, Riccardi V, Samango-Sprouse C, Ferner R, Moore B, Legius E, et al. Cognitive function and academic performance in neurofibromatosis 1: consensus statement from the NF1 Cognitive Disorders Task Force. Neurology. 1997;48:1121–1127.
3. North K, Joy P, Yuille D, Cocks N, Hutchins P. Cognitive function and academic performance in children with neurofibromatosis type 1. Dev Med Child Neurol. 1995;37:427–436.
4. North K, Joy P, Yuille D, Cocks N, Mobbs E, Hutchins P, et al. Specific learning disability in children with neurofibromatosis type 1: significance of MRI abnormalities. Neurology. 1994;44:878–883.

5. Rauen KA, Schoyer L, McCormick F, Lin AE, Allanson JE, Stevenson DA, et al. Proceedings from the 2009 genetic syndromes of the Ras/MAPK pathway: From bedside to bench and back. Am J Med Genet. A 2010;152A(1):4-24.
6. Li, W, Cui Y, Kushner SA, Brown RA, Jentsch JD, Frankland PW, et al. The HMG-CoA reductase inhibitor lovastatin reverses the learning and attention deficits in a mouse model of neurofibromatosis type 1. Curr Biol. 2005;15:1961–1967.
7. Kaplan AM, Chen K, Lawson MA, Wodrich DL, Bonstelle CT, Reiman EM. Positron emission tomography in children with neurofibromatosis-1. J Child Neurol. 1997;12:499–506.
8. Balestri P, Lucignani G, Fois A, Magliani L, Calistri L, Grana C, et al. Cerebral glucose metabolism in neurofibromatosis type 1 assessed with [18F]-2-fluoro-2-deoxy-D-glucose and PET. J Neurol Neurosurg Psychiatry 1994;57:1479–1483.
9. Gérard N, Pieters G, Goffin K, Bormans G, Van Laere K. Brain type 1 cannabinoid receptor availability in patients with anorexia and bulimia nervosa. Biol Psychiatry. 2011;70(8):777-84.
10. Ginger ALE. Available: http://www.brainmap.org/ale/index.html.
11. Talairach Client. Available : http://www.talairach.org/manual.html.
12. Buchert R, von Borczyskowski D, Wilke F, Gronowsky M, Friedrich RE, Brenner W et al. Reduced thalamic 18F flurodeoxyglucose retention in adults with neurofibromatosis type 1. Nucl Med Commun. 2008;29(1):17-26.
13. Van Bogaert P,Wikler D, Damhaut P, Szliwowski HB, Goldman S. Regional changes in glucose metabolism during brain development from the age of 6 years. Neuroimage. 1998;8:62–68.
14. Cho ZH, Son YD, Kim HK, Kim NB, Choi EJ, Lee SY et al. Observation of glucose metabolism in the thalamic nuclei by fusion PET/MRI. J Nucl Med. 2011;52(3):401–404.
15. Watanabe Y, Funahashi S. Thalamic mediodorsal nucleus and working memory. Neurosci Biobehav Rev. 2012;36(1):134-42.
16. Hyman SL, Shores A, North KN. The nature and frequency of cognitive deficits in children with neurofibromatosis type 1. Neurology. 2005;65:1037–1044.
17. Herholz K, Ehlen P, Kessler J, Strotmann T, Kalbe E, Markowitsch HJ. Learning face-name associations and the effect of age and performance: a PET activation study. Neuropsychologia. 2001;39(6):643-50.
18. Huijbregts S, Jahja R, De Sonneville L, de Breij S, Swaab-Barneveld H. Social information processing in children and adolescents with neurofibromatosis type 1. Dev Med Child Neurol. 2010;52(7):620-5.
19. Hazlett EA, Buchsbaum MS, Hsieh P, Haznedar MM, Platholi J, LiCalzi EM et al. Regional glucose metabolism within cortical Brodmann areas in healthy individuals and autistic patients. Neuropsychobiology. 2004;49(3):115-25.
20. Gillberg C, Forsell C. Childhood psychosis and neurofibromatosis—more than a coincidence? J Autism Dev Disord. 1984;14(1):1–8.
21. Marui T, Hashimoto O, Nanba E, Kato C, Tochigi M, Umekage T et al. Association between the neurofibromatosis-1 (NF1) locus and autism in the Japanese population. Am J Med Genet B Neuropsychiatr Genet. 2004;131B(1):43-7.
22. Feldmann R, Denecke J, Grenzebach M, Schuierer G, Weglage J. Neurofibromatosis type 1: motor and cognitive function and T2-weighted MRI hyperintensities. Neurology. 2003;61(12):1725–1728.
23. Goh WH, Khong PL, Leung CS, Wong VC. T2-weighted hyperintensities (unidentified bright objects) in children with neurofibromatosis 1: Their impact on cognitive function. J Child Neurol. 2004;19:853–8.

24. Moore BD, Slopis JM, Schomer D, Jackson EF, Levy BM. Neuropsychological significance of areas of high signal intensity on brain MRIs of children with neurofibromatosis. Neurology. 1996;46:1660–8.
25. Hyman SL, Gill DS, Shores EA, Steinberg A, North KN. T2 hyperintensities in children with neurofibromatosis type 1 and their relationship to cognitive functioning. J Neurol Neurosurg Psychiatry. 2007;78(10):1088-91.
26. Hyman SL, Gill DS, Shores EA, Steinberg A, Joy P, Gibikote SV et al. Natural history of cognitive deficits and their relationship to MRI T2-hyperintensities in NF1. Neurology. 2003;60(7):1139–1145.
27. Muzik O, Chugani DC, Juhász C, Shen C, Chugani HT. Statistical parametric mapping: assessment of application in children. Neuroimage. 2000;12(5):538-49.
28. Zhang J, Mitsis EM, Chu K, Newmark RE, Hazlett EA, Buchsbaum MS. Statistical parametric mapping and cluster counting analysis of [18F] FDG-PET imaging in traumatic brain injury. J Neurotrauma. 2010;27(1):35-49.
29. Kessler RM, Ellis JR Jr, Eden M. Analysis of emission tomographic scan data: limitations imposed by resolution and background. J Comput Assist Tomogr. 1984;8:514–522.
30. Moore BD 3rd, Slopis JM, Jackson EF, De Winter AE, Leeds NE. Brain volume in children with neurofibromatosis type 1: relation to neuropsychological status. Neurology. 2000;54:914–920.
31. Chen WP, Samuraki M, Yanase D, Shima K, Takeda N, Ono K et al. Effect of sample size for normal database on diagnostic performance of brain FDG PET for the detection of Alzheimer's disease using automated image analysis. Nucl Med Commun. 2008;29(3):270-6.
32. Kiyama Y, Ito K, Kato T, Tamaki T, Nishio M, Tamai S, et al. Characteristics of FDG brain images obtained in whole PET body scan in an aspect of statistical image analyses. J Nucl Med. 2007;48 (Suppl. 2):461P.
33. Pappius HM, Wolfe LS. Effects of indomethacin and ibuprofen on cerebral metabolism and blood flow in traumatized brain. J Cereb Blood Flow Metab. 1983;3(4):448-59.
34. Pinkofsky HB, Dwyer DS, Bradley RJ. The inhibition of GLUT1 glucose transport and cytochalasin B binding activity by tricyclic antidepressants. Life Sci. 2000;66(3):271-8.

Peer-review history:
The peer review history for this paper can be accessed here:
http://www.sciencedomain.org/review-history.php?iid=205&id=12&aid=1415